Magicol: Indoor Localization Using Pervasive Magnetic Field and Opportunistic WiFi Sensing

Yuanchao Shu, *Student Member, IEEE*, Cheng Bo, Guobin Shen, *Senior Member, IEEE*, Chunshui Zhao, Liqun Li, and Feng Zhao, *Fellow, IEEE*

***Abstract*—Anomalies of the omnipresent earth magnetic (i.e., geomagnetic) field in an indoor environment, caused by local disturbances due to construction materials, give rise to noisy direction sensing that hinders any dead reckoning system. In this paper, we turn this unpalatable phenomenon into a favorable one. We present Magicol, an indoor localization and tracking system that embraces the local disturbances of the geomagnetic field. We tackle the low discernibility of the magnetic field by vectorizing consecutive magnetic signals on a per-step basis, and use vectors to shape the particle distribution in the estimation process. Magicol can also incorporate WiFi signals to achieve much improved positioning accuracy for indoor environments with WiFi infrastructure. We perform an in-depth study on the fusion of magnetic and WiFi signals. We design a two-pass bidirectional particle filtering process for maximum accuracy, and propose an on-demand WiFi scan strategy for energy savings. We further propose a compliant-walking method for location database construction that drastically simplifies the site survey effort. We conduct extensive experiments at representative indoor environments, including an office building, an underground parking garage, and a supermarket in which Magicol achieved a 90 percentile localization accuracy of 5 m, 1 m, and 8 m, respectively, using the magnetic field alone. The fusion with WiFi leads to 90 percentile accuracy of 3.5 m for localization and 0.9 m for tracking in the office environment. When using only the magnetism, Magicol consumes 9× less energy in tracking compared to WiFi-based tracking.**

***Index Terms*—Indoor localization, map construction, magnetic field, opportunistic WiFi.**

I. Introduction

ACCURATE and pervasive indoor positioning can significantly improve our everyday life. Examples include local searching for position of interest (POIs) in a shopping mall, navigating to a meeting room in an unfamiliar office building, and finding a car in a parking garage. WiFi [1]–[4], cellular [5]–[7], or even FM [8], [9] based approaches have shown great promise but may not be as effective when the signals are weak or not available, as is the case in an underground parking garage. The WiFi scans are also known to be energy expensive.

The (geo-)magnetic field is omnipresent, and thus can potentially be leveraged for a pervasive positioning technology for an indoor environment without any dependency on infrastructure. There are several ways to exploit the geomagnetism for localization purposes. One is to obtain the walking direction from the magnetic field, typically used in an inertial sensor based tracking (i.e., dead reckoning) system [10]–[12]. However, the direction sensing inside a building is extremely noisy due to the geomagnetic field anomalies caused by the local disturbances of ferromagnetic building materials [13], [14]. Another way, in contrast, is to exploit the magnetic field anomalies as distinctive signatures. But these systems either require customized hardware [15] or work under specific scenarios [16], [17]. The magnetic field anomalies are also used to discriminate indoor and outdoor environment in [18], and as indoor landmarks in [12].

In this paper, we present the design and evaluation of *Magicol*—a magnetic field based indoor localization and tracking system for smartphone users. Recognizing that *the indoor geomagnetic field anomalies are omnipresent, location specific and temporally stable*, Magicol leverages the locally disturbed magnetic signals as location-specific signatures. It uses the magnetometer commonly found on smartphones, without resorting to special hardware. Through magnetic sensing that consumes very little energy, Magicol is energy efficient and applicable to almost every indoor venue.

To make Magicol a reality, we must address three major challenges. First, the magnetic signal has a very limited discernibility. A single observation cannot be reliably used as a unique location signature. In Magicol, we leverage user motion to *vectorize* multiple observations to form a higher dimensional signature. This vector is then matched against a pre-established magnetic signal map (M-Map), a location database built offline with mappings between magnetic signals and their locations, to localize the user. A user may walk arbitrarily, in different directions and with different strides, and may stop from time to time. To ensure tractable complexity, the vectorization is performed on a per-step basis, and the matching process is realized through an augmented particle filter (APF) in which the similarity between the signal vector and that in the M-Map is used to weigh particles. We design a novel *map-constrained, position-aware, and inertial-based* (MPI) particle motion model to avoid using absolute (indoor) heading directions that are known to be noisy. We further use dynamic time warping in APF to address practical issues such as variations in spatial sampling density, devices, and usage patterns.

Manuscript received July 31, 2014; revised November 30, 2014; accepted February 16, 2015. Date of publication May 6, 2015; date of current version June 22, 2015.

Y. Shu is with the Department of Control Science and Engineering, Zhejiang University, Hangzhou 310027, China (e-mail: ycshu@zju.edu.cn).

C. Bo is with University of North Carolina at Charlotte, Charlotte, NC 28223 USA (e-mail: cbo@hawk.iit.edu).

G. Shen, C. Zhao, and F. Zhao are with Microsoft Research Asia, Beijing 100080, China (e-mail: jackysh@microsoft.com; chunzhao@microsoft.com; zhao@microsoft.com).

L. Li is with PPzuche.com, Beijing 10011, China (e-mail: liqul@outlook.com).

Color versions of one or more of the figures in this paper are available online at http://ieeexplore.ieee.org.

Digital Object Identifier 10.1109/JSAC.2015.2430274

Secondly, while Magicol works without dependency on a WiFi infrastructure, but it can work even better in dense WiFi AP deployment environments, an issue that has not been exploited. We show the WiFi and magnetic signals are indeed complementary: WiFi signals are distinctive across distant locations whereas magnetic field are more locally discriminative. We then explore a few intuitive ways of magnetic-WiFi fusion, which uses a rough WiFi localization estimate to confine initial particle distribution and also considers the WiFi fingerprint similarity in the course of APF. In particular, we design a *two-pass, bidirectional* particle filtering method to fuse the WiFi and magnetic localization. Given a WiFi scan result and a background logged motion trace with unknown starting position, the first pass aims to obtain a good estimate of the starting position via backward particle filtering on the reversed motion trace with particles initially distributed around the WiFi-based location estimate. The resultant starting position is in return used to ensure better initialization of the forward particle filtering process in the second pass.

Thirdly, as in radio based localization systems, the location database (i.e., M-Map in Magicol) needs to be constructed in advance. This is a non-trivial problem and has been actively studied recently [19], [20]. In addition, the low discernibility of the magnetic field entails a densely collected database. We propose a *compliant-walk* (CW) based site survey solution. A surveyor only needs to walk normally along pre-planned survey paths. The phone collects inertial sensor readings and magnetic signals automatically during the walk. The system estimates the actual walking traces from the sensor data, and matches the data against the paths through dynamic programming. This fixes the positions of the steps, from which positions of magnetic signals are interpolated. With CW, the survey task is significantly simplified for an ordinary phone user. This method is also applicable to other localization means such as WiFi-based fingerprinting.

In summary, the contributions of Magicol are threefold:

- We perform an in-depth study of the indoor magnetic field properties and propose effective techniques to exploit the anomalies of the magnetic field for localization and handle several practical challenges.
- We propose a novel two-pass bidirectional particle filtering process to fuse magnetic and WiFi signals for more accurate indoor positioning and tracking.
- We devise a compliant-walk based location database construction method which significantly lowers the bar for ordinary smartphone users to conduct site surveys.

We have carried out extensive experiments to evaluate the performance of Magicol under three representative indoor environments, an office floor, an underground parking garage, and a supermarket. Magicol achieves high positioning accuracy: a 90 percentile localization accuracy of 5 m, 1 m, and 8 m in the three environments, using magnetic field alone. We note the WiFi AP deployment is very sparse in the underground parking garage and supermarket. Therefore, we study the localization accuracy for magnetic and WiFi fusion in the office building only. The results confirm that, using magnetic field alone, Magicol achieves comparable accuracy with WiFi-based approaches (i.e., EZ [3] and Radar [1]), and that the fusion with WiFi leads to a 90 percentile accuracy of 3.5 m for localization and 0.9 m for tracking. We profiled the energy consumption for Magicol clients. Magicol is 9× more energy efficient when tracking with magnetism than a pure WiFi-based solution.

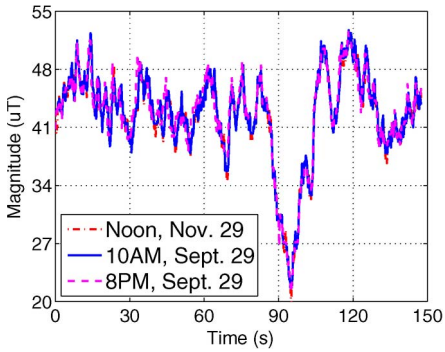

Fig. 1. Stable and locally disturbed indoor geomagnetic field. Measurement was on a straight corridor, at different time of day and different days.

II. Insight on Geomagnetism

In this section, we provide some measurement study on the properties of the indoor magnetic field, some are favorable for indoor localization purpose, whereas others bring challenges to actual exploration.

A. Favorable Geomagnetic Field Properties

Locally Disturbed yet Stable Magnetic Field: Indoor magnetic fields have been found to exhibit certain anomalies due to the disturbances caused by building construction materials and electrical appliances. The patterns of disturbance are different across different locations. In addition, the magnetic field, including the local disturbances, is very stable over time as long as the internal layout remains unchanged. Fig. 1 clearly demonstrates these properties, where the magnetic signals were collected during walks along a straight corridor in an office building at different times of day, and on two different dates that were two months apart. The local disturbance and the stability over time make the magnetic field a potential candidate for localization purpose. We note that it has been reported and preliminary explored in many previous work (e.g., [13]–[15], [17], [18], [21]–[24]), we include them here for completeness.

Limited Impact of Mobile Objects: Indoor environments are usually highly dynamic, due to mobile objects such as people, cars, elevators, and on/offs of electrical appliances. We studied the impact they have on the magnetic field in typical scenarios. The results are shown in Fig. 2. Fig. 2(a) shows the impact of cars, with data having been collected along the red line that was about 1 meter away from the car. We collected data twice: at 4PM when the garage was full of cars, and at 12AM when the garage was almost empty. We can see that cars have little impact on the magnetic field that is 1 meter away. We also measured the influences of people and grocery carts in a supermarket.

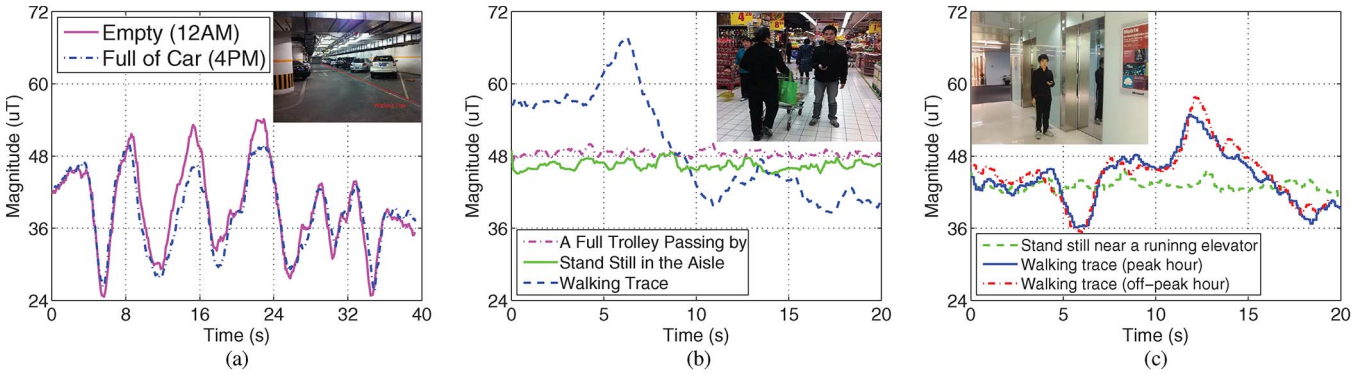

Fig. 2. Measurement of the impact of mobile objects on the magnetic field. (a) Underground parking lot. (b) Supermarket. (c) The elevator lobby.

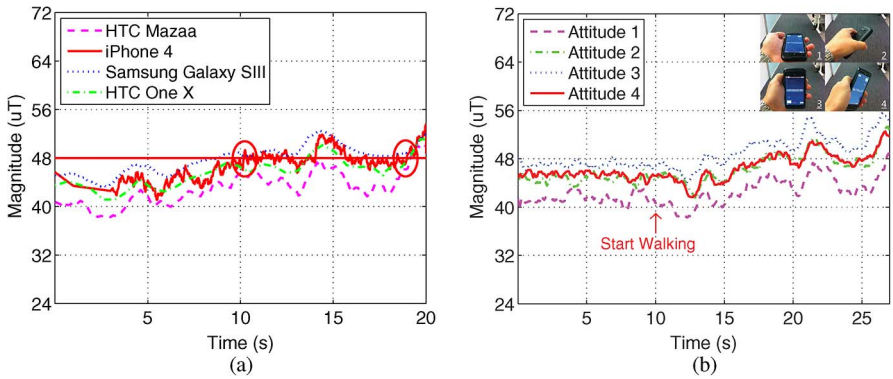

Fig. 3. Magnetic field measurement results with (a) different mobile phones, and (b) different attitudes for the same phone.

As can be seen in Fig. 2(b), there was no visible impact from trolleys and people walking by. On the contrary, the fluctuation of magnetic measurement is much larger and obvious during user walking. We also collected magnetic signals in an elevator lobby with 12 running elevators at a 1-meter distance from the elevator doors. In Fig. 2(c), comparing with drastic fluctuations of magnetic values during walking, running elevators do not bring serious impacts when the user is standing still. That means the elevator infrastructure had a more significant impact on the magnetic field whereas the moving cabin had little impact. In summary, our experiments confirm that the impact of mobile objects is very limited, and have barely no impact at a distance of one meter away.

B. Challenges in Using the Magnetic Field

Low Discernibility of Magnetic Signals: The strength of (geo-)magnetic field is usually very weak, commonly within a few tens of uT. Hence, single magnetic signal offers very limited discernibility. Taking the iPhone 4 trace shown in Fig. 3(a) as an example. If we randomly pick one magnitude, say 48, we will find many locations with magnitude 48 in the rather short trace.

The magnetic field is directional, and a magnetometer measures 3-D magnetic signals. It is natural to think of using the 3-D signal to increase the discernibility. However, it is hard to do so in practice because the frame of reference of the magnetometer may not always align with the global coordinate system. To ensure the alignment, it would require either to accurately track the device attitude all the time or to constrain the device usage to some fixed attitude (e.g., hand-held horizontally with Y-axis towards heading direction). The former is difficult due to sensor drift and the latter severely affects user experiences. Therefore, only the magnitude of the magnetic signal may be used in practice.

Device Diversity and Usage Diversity: We found that for the same magnetic field, different devices will show different readings. This is clearly demonstrated in Figs. 3 and 4. Fig. 3(a) shows the magnitude of the collected magnetic signals along exactly the same path using different smartphones. For the same device, if the data was collected at different device attitudes, then the resulting signals vary. This is confirmed in Fig. 3(b), where the data was collected with different attitudes along the same path. Note that during the experiments, we stood still for 10 seconds before walking to discriminate sensor noise and magnetic field variation. Such diversity in terms of devices and usage further impair discernibility.

Statistical results of the deviation of magnetic field measurement are shown in Fig. 4. In Fig. 4 we can see that compared with temporal influence, deviations of magnetic measurement among different devices and attitudes are larger. However, deviation values are relatively stable with different trace lengths, and variances of deviation are small that result in steep slopes of all three CDF curves.

As a brief summary, the magnetic field has favorable intrinsic properties (i.e., stability and local disturbance) to serve as a localization modality. However the low discernibility of

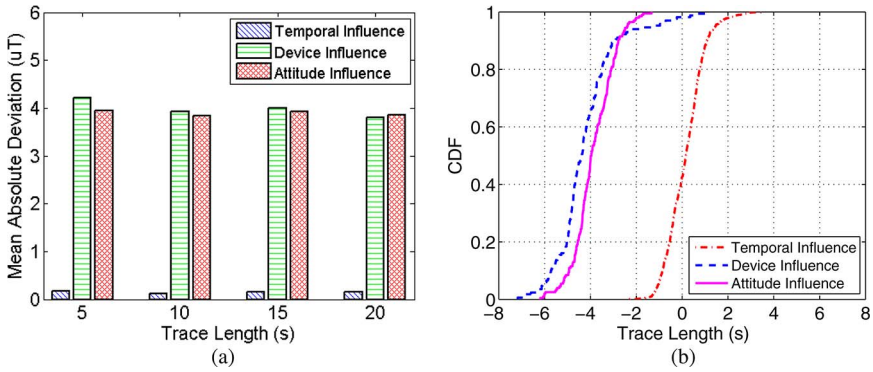

Fig. 4. Statistical results of the deviation of magnetic field measurement. (a) Mean absolute deviation. (b) CDF of the deviation.

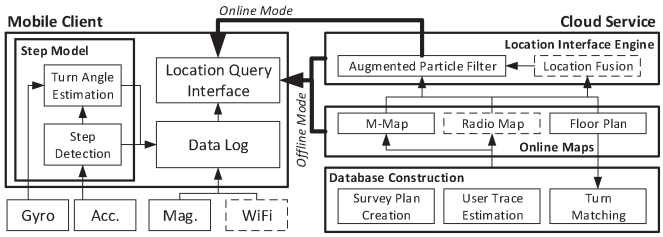

Fig. 5. Magicol architecture.

magnetic signals make it rather challenging to explore the magnetic signal directly, e.g., using fingerprinting techniques.[1] The device and usage diversities further pollute the sensed magnetic strength.

III. Magicol Overview

The insights into indoor geomagnetism indicate both opportunities and challenges when utilizing a magnetic field for localization purposes. On one hand, features such as the ubiquitousness, the location-specific, temporally stable and undisturbed anomalies clearly reveal the potential of using magnetic signals as location signatures. On the other hand, the low discernibility, device and usage diversity impose real challenges that we need to overcome.

In this section, we provide an overview of Magicol—an indoor localization system for mobile phone users that exploits the globally available geomagnetic field. Magicol consists of a mobile client and a backend Cloud service. The mobile client has two operating modes: online and offline. The overall architecture of Magicol is depicted in Fig. 5.

Mobile Client: The Magicol client performs *background* data logging (to facilitate immediate localization) of IMU sensor data and, opportunistically, the WiFi sensing results. To save memory and communication costs, it performs motion state detection and keeps a window of the most recent walking information (e.g., step length, turning angle of the step) and the corresponding magnetic signals. Walking state detection is well studied and we employ the step detection techniques and personalized step model developed by Li *et al.* [25]. The mobile client may operate in online mode if network access is available. In this mode, the background logged data is sent to the Cloud service to obtain a location fix; it may also operate in offline mode when there is no network access and the location database is downloaded beforehand. In this mode, the location is resolved locally on the device using a local location inference engine.

Cloud Service: Cloud service consists of two subsystems: location database construction and a location inference engine. The location database consists of the magnetic fingerprint map (M-Map) that contains <position, magnetic field strength> tuples and the radio map which stores the WiFi information. The *M-Map construction* subsystem solves the location database construction problem through a simple yet efficient *compliant-walking-based* (CW) site surveying method (Section VI). The subsystem further consists of three modules: survey plan creation, user trace estimation, and trace matching.

The location inference engine receives and resolves location queries from mobile clients. As a common module for both the mobile client (in offline mode) and the backend Cloud service, it resolves a user's location by matching the magnetic signals against the M-Map. The location resolution process is achieved through an *augmented particle filter* that operates on a per-step basis (Section IV). Depending on the availability of other opportunistically sensed signals (e.g., WiFi), it may leverage and fuse them with the magnetic field-based localization process (Section V).

IV. Tracking With Magnetic Field

In this section, we present the tracking engine that resolves user's location through observed magnetic signals and the IMU data using particle filtering. In addition to aforementioned low discernibility of the magnetic signal, device and usage diversities, it further faces challenges caused by different spatial sampling density due to different walking speed or sensor sampling rate. We elaborate concrete techniques that overcome all these challenges.

[1]We note that fingerprinting technique was successfully applied in [15], where a customized device with a plural of sensors was used. As only one device is used with attitudes kept the same in experiments, the diversities was not recognized nor handled.

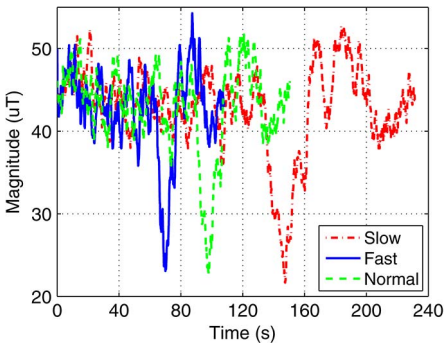

Fig. 6. Traces for the same path at different walking speeds.

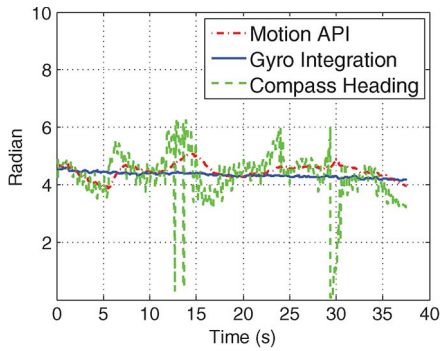

Fig. 7. Headings from compass, gyroscope and fusion (motion API), for an indoor straight walking. Gyro gives relative direction changes and is offset from 0 to around 4 radian (the corridor direction) for easier view.

A. Step-Based Vectorization

To improve the discernibility of (geo-)magnetic signals, one common method is to increase the spatial coverage of measurements. Unlike [15] where the authors obtained a 12-D vector magnetic signal using a special customized hardware, which implies not applicable to mobile phones, we propose to *vectorize* multiple temporal observations into a high dimensional vector signal. This vector signal has increased spatial coverage due to *the fact that the user is walking*. Let's again take Fig. 3(a) as an example. Now suppose the device observes three consecutive samples with magnitude {47, 48, 49}. There are only two possible locations (highlighted with red circles) with similar observations. The discernibility is indeed improved. Obviously, the longer the trace we vectorize, the more discriminative the resulting vector signal will be.

We incorporate the step model and vectorize all the samples *within the same step* as a vector for three reasons. First, when performing a vector comparison, it makes sense only when both vectors cover a similar spatial distance. Thus, we need to have an estimate of the spatial coverage of the step vector. Such information is readily available from IMU-based tracking. Second, all the samples within the same step always have the same motion direction. This is the fundamental reason that we can combine them into one vector. Third, using step model naturally handles the discontinuity in the walking process.

B. Magnetic Vector Matching With DTW

The magnetic field is sampled continuously while walking. Due to possibly different walking speeds and different sampling rates, different number of samples may result for the same spatial coverage. We refer to this as *spatial sampling density variation* issue. Fig. 6 demonstrates this problem. In our experiments, we walked along the same path at different speeds while sampling the magnetometer at a fixed frequency. We found that fast walking led to shorter traces and fewer samples, whereas slow walking yielded long traces and more samples. This translates to different spatial sampling density because the walks covered the same path. Different temporal sampling frequencies will further complicate the phenomenon.

The spatial sampling density variation makes it difficult to directly compare two vectors that cover the same spatial range, as they are likely to have different dimensionalities. However, a closer look at Fig. 6 reveals that, despite the different spatial sampling densities, their shapes look similar. Therefore, in Magicol, we adopt dynamic time warping (DTW) to compare two vectors. DTW is a proven effective algorithm for measuring similarity between two sequences that may vary in time or speed.

Handling the Diversities: We further handle the device diversity and usage diversity issues, identified in Section II, with a simple mean removal technique: both the signal vector and the candidate vector have their mean removed before applying DTW. The rationale is that, despite the diversities in measured magnetic strengths, the shape of the resulting magnetic signal sequences are all similar for the same path, as confirmed in both Figs. 3 and 6. Therefore, we can rely on the shape of the local magnetic field instead of their absolute values.

In brief, to match a magnetic signal vector collected in one step, we compose a mean-removed candidate vector in the database. The candidate vector consists of a set of successive geomagnetic samples spread over the travelling path of each particle. These samples cover the same spatial distance of that step. We then remove the means of both the measurement vector and the candidate vector, and apply DTW to calculate their similarity.

C. Particle Motion Model

Particle filtering is commonly adopted in tracking applications. In these work, particles are *uniformly* driven by *externally* sensed absolute heading directions, which is often the fusion result from compass and gyroscope. However, due to the magnetic field anomalies, the heading direction, even after fusion, is still very noisy, as evidenced in Fig. 7.

Magicol also adopts particle filtering. Unlike existing tracking systems that fuse the magnetometer and the gyroscope to obtain a compromised result, Magicol makes separate use of them to best exploit the strength of each sensor modality: the gyroscope can reliably tell relative walking direction; magnetic field anomalies can serve as useful location features.

Based on the observation that a user is very likely to follow the main direction of the path and is very likely to continue walking in a consistent direction rather than making random turns, we come up with a *map-constrained, position-aware,*

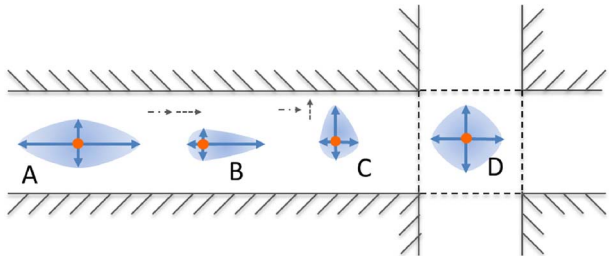

Fig. 8. Illustration of the map-constrained, position-aware, inertial-based particle motion model. The likelihood of particle's direction is jointly determined by its position on the map and its direction in the previous step.

inertial-based (MPI) particle motion model to drive particles. In this MPI motion model, as illustrated in Fig. 8, the direction $\vec{u}$ of a newborn particle (e.g., Particle A and D) is determined by the direction $\vec{u}_{pw}$ of the pathway it is on; and that of a resampling particle (e.g., Particle B and C) is that of the previous step plus the relative direction change $\vec{u}_{gyro}$ during this step, hence the term *inertial-based*. The relative direction is obtained from the gyroscope using the technique presented in Section VI.

Note that the gyroscope may occasionally give a false positive conclusion of turns due to the possibility of sudden attitude change (e.g., change holding hands), but it seldom misses the detection of real turns. Therefore, if the gyroscope indicates no turn, we may significantly reduce (or even eliminate) the possibility of a direction turn (e.g., Particle B); whereas when the gyroscope indicates a turn, we will increase the probability of a turn in direction but still retain a certain probability of the original direction (e.g., Particle C). If the turn indication is a false alarm, then the particles will soon hit the wall and die. Clearly, Magicol makes more use of the map information than existing tracking systems. It uses not only the walls to kill incorrectly moved particles, but also uses the pathway directions to better initialize a particle's direction.

D. Augmented Particle Filter

All these techniques are combined into an augmented particle filter that executes on a per-step basis. The state of a particle includes its current location $\vec{p} = \{x, y\}$ and also the heading direction $\vec{u}$. The observations are obtained from the mobile client, include step information (step length, relative direction change) and the magnetic fingerprint vector collected during the step.

Particle Movement: With new step input, location of each particle is updated as follows:

$$\vec{u}' = \begin{cases} P(\vec{u}_{pw}) & \text{for newborn particles} \\ \vec{u} + \vec{u}_{gyro} + \Delta\vec{u} & \text{for resampling particles} \end{cases} \quad (1)$$

$$p'.pos = p.pos + (l + \delta) \cdot \vec{u}' \quad (2)$$

where $P(\vec{u}_{pw})$ is a probabilistic selection function that instantiates the direction of a newborn particle according to its position. $\Delta\vec{u}$ accounts for possible direction errors that are also assumed to follow a Gaussian distribution with zero mean and variance set to 10°. l is the estimated step length and δ obeys a Gaussian distribution with zero mean and variance set to $0.2l$ to capture the possible error of step length estimation.

Particle Weight Assignment: The weight of a particle is set to

$$\kappa = e^{-\frac{d^2}{2\sigma^2}} \quad (3)$$

where d is the resulting DTW distance and σ is a parameter that reflects the overall disturbance intensity of the indoor magnetic field. Particularly, if a particle hits a wall, its weight will be significantly reduced ($\times 0.01$, but not eliminated).

Particle Resampling: Once after particle weight updating, we conduct weight-based importance sampling over the entire set of particles. This way, particles moving at wrong directions will eventually be killed as the mismatches between the magnetic signals will continuously reduce their weight.

Position Decision Strategy: The distribution of particles reflects the likelihood of the real position. There two common ways to determine the position from particle distribution: one is to use the position of the particle with maximum weight; the other is to perform a weighted average on all particles' positions using their own weights. Through experiments, we found that the former method locks on the user more quickly but may fluctuate more during the tracking process, whereas the latter method takes longer time to lock on but gives more steady position during tracking. In Magicol, we use a hybrid method: initially go after the particle with maximum weight, and switch to weighted average once it converges. We use the weighted average of top 50% most weighted particles.

V. Fusion With WiFi

Tracking using only the magnetic field and inertial sensors is universally applicable. However, given the wide deployment of WiFi, we may obtain both WiFi and magnetic signals simultaneously in many venues. In this section, we study the fusion of WiFi and magnetic signal towards even better positioning and tracking accuracy.

A. Rationale of Fusion

The fundamental reason that Magicol can be combined with a WiFi-based localization method lies in their complementary location resolving capabilities. Conceptually, WiFi is a short range radio. It is guaranteed that remote locations will see different radio environment (less or no common APs), whereas nearby locations will share similar radio environment. On the contrary, the geomagnetic field is global. Remote locations may have similar magnetic fields, whereas nearby locations may have different ones due to the local disturbance to the magnetic field.

This concept is better illustrated in Fig. 9, which shows the normalized distances in the signal space between every pair of locations sequentially sampled from two distant parallel corridors. From Fig. 9(a), we can see that the distances between neighboring locations can be large for those locations where the magnetic field is indeed disturbed. However, distant locations may also observe similar magnetic signals, especially when their magnetic fields are less disturbed. On the other hand, as shown in Fig. 9(b), WiFi signals are usually similar for nearby locations, but quite different for faraway locations. If we consider both the magnetic and the WiFi signals, the resulting

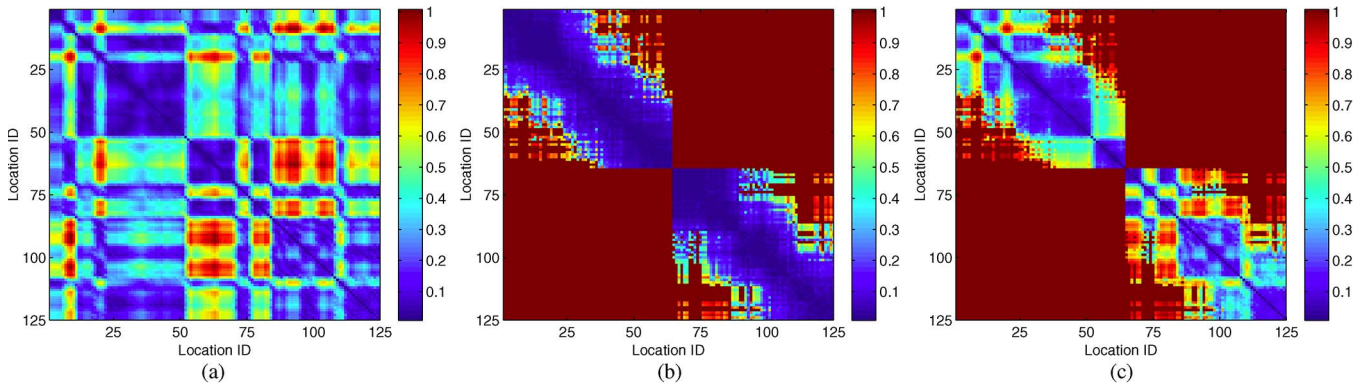

Fig. 9. The Manhattan distance of signal vectors between all pairs of profiled locations in a large mall. Location 1–65 are from one corridor and location 66–125 are from the other. (a) Magnetic. (b) WiFi. (c) Magnetic + WiFi.

distances (in the signal space) will be a blend of the two signals, as evidenced in Fig. 9(c). This clearly indicates the potential of combining the WiFi and magnetic signals.

B. Intuitive Fusion Methods

Given the complementary properties of magnetic field and WiFi, it is natural to think of a few possible ways to fuse them. The first way is to use WiFi for a rough position estimation and constrain particle distribution to a proximity of the WiFi location estimate. This is particular helpful at the initial of tracking and lead to faster convergence. The second way is to incorporate the similarity of WiFi signals to weigh particles during the filtering process. For instance, the weight of a particle is set to

$$\kappa = e^{-\frac{d_m^2}{2\sigma_m^2}} + e^{-\frac{d_w^2}{2\sigma_w^2}} \tag{4}$$

where d_m and d_w are the distance in signal space for the magnetic and WiFi signals, respectively. σ_m and σ_w are parameters adjusting the impact of signal distances. A third way is to hybrid the first two by weighing particles with both signal modalities but also constrain the particle distribution to be within a proximity of WiFi location estimate.

C. Fusion for Better Accuracy

It is well known that the WiFi localization results are jumpy—measurements of two neighboring positions can lead to quite different actual position estimates. This affects the performance of fusion using the intuitive methods presented above. To achieve better accuracy, we propose a *two-pass bidirectional particle filtering* (TBPF) process to fuse WiFi and magnetic signals during tracking, where magnetic signals are available (e.g., logged in the background) when a WiFi scan is performed. The cost we pay is more computation.

Two-Pass Bidirectional Particle Filtering: Fig. 10 illustrate the TBPF process. In the first pass, we first obtain the rough location estimate P_0 using WiFi signals, and apply a *backward* particle filtering along the *reversed* motion trace. In this pass, the hybrid fusion scheme mentioned above is adopted. The locality-preserving property of WiFi guarantees the true position to be near P_0. Therefore, we distribute initial particles only within a proximity of P_0, i.e., a circle centered at P_0 with radius R. With the backward particle filtering process, we obtain a good estimate of the starting position P_t of the logged trace. In the second pass, we perform a *forward* particle filtering along the motion trace normally, but initialize all the particles to be within a circle around P_t with radius r. Finally, we perform a post-filtering process and retain only the particles that fall within the range R' to P_0. The weighted average of these particles and obtain the final localization result P'_0.

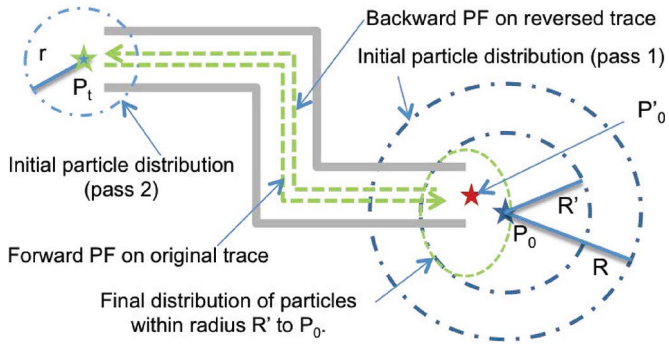

Fig. 10. Illustration of the two-pass bidirectional particle filtering process.

Note that the same background logged motion trace are used twice in the TBPF. This makes the particle filtering in the second pass biased. In general, the bias will lead to either better or worse results. It is thus *crucial* to apply the final post-filtering process (i.e., selecting particles within radius R' to P_0). This selection implicitly uses some truth information—the true location must be around P_0, and ensures the bias is favorable.

VI. M-Map Construction

The conventional site survey approach suffers from low efficiency as the surveyor needs to first fix the location before collecting any sensor readings. SLAM techniques (either employing robots [26] or via crowdsourcing [19], [20]) suffer from poor initial accuracy and slow convergence. We believe that site survey is an effective method because the surveyor is more dedicated to the task. Our idea is to lower the bar such that ordinary mobile phone users can do the survey job at high efficiency.

To this end, we devise a simple *compliant-walking-based* data collection method: the surveyor simply walks along a pre-planned survey path from the starting point to the end point with the phone in a fixed body position. The system records all the IMU data including accelerations, gyroscope readings, and magnetic signals from the magnetometer during the walk. The actual user trace is then estimated and matched against the pre-planned path to fix the location of each step. Then locations of all collected magnetic signals are interpolated from neighboring step positions.

Note that here we focus on the design of the *compliant-walking-based* site survey method. Businesses that wish to build an indoor location system can utilize crowdsourcing or outsource the survey task to crowd tasking platforms, such as Amazon Mechanical Turk [27] to quickly bootstrap their services. We leave the design of incentive models of site survey as our future work.

Survey Plan Creation: Given a venue map, we need to first come up with a survey plan that covers all paths (of interest). It can be generated manually or following some simple rule such as a right-hand or left-hand wall follower rule [28]. Considering the spatial coverage, the path is through the middle for narrow pathways, whereas for extra wide path segments or open spaces, we add additional survey paths that are parallel to the middle one but separated by about 3 meters. This is empirically determined by experiments and is supported by the achievable accuracy of Magicol shown in Section VII.

Walking Trace Estimation: Walking trace estimation using IMU sensors is a well-studied topic. The estimation consists of step detection, step length estimation, and step direction estimation. We adopt the techniques used in [25]. However, instead of inferring the heading direction from the magnetometer, we estimate the relative heading direction change in that step using gyroscope. As the device may be put in any attitude, we convert the sensor readings from the device's body frame to its vehicle-carried North East Down (NED) frame [29], which is close to the local World Coordinate System. The conversion matrix is obtained by estimating the gravity in the device's body frame by taking the average acceleration over the past several steps. Since the turning action always happen along the horizontal plane that is perpendicular to the gravity, we can estimate the turning angle by integrating the Z-axial rotation in the vehicle-carried NED frame. A negative or positive turning angle indicates a direction change towards the left or right, regardless of the device's actual attitude.

Turn Detection: We apply a running detection window (empirically set to 7 steps) to the resulting walking traces. We identify a candidate turn if the sum of the angle changes within the detection window exceeds a threshold, say 30 degrees. A real turn may lead to multiple candidate turns. We further merge the consecutive turns and perform a local search such that any additional steps belonging to the same turn are included. This ensures the integrity of the turn and improves the detection accuracy of the turning angle. The turning point is set at the step with the sharpest angle changes.

Trace Matching via Dynamic Programming: We match an estimated user trace to its corresponding pre-planned path by first matching the turns because the turns are the most salient features of a user trace. We have two lists of turns: one ground truth turn list ($\mathcal{G}$) obtained from the pre-planned paths and one candidate turn list ($\mathcal{C}$) from the estimated user traces. Taking Fig. 11 as an example, we have

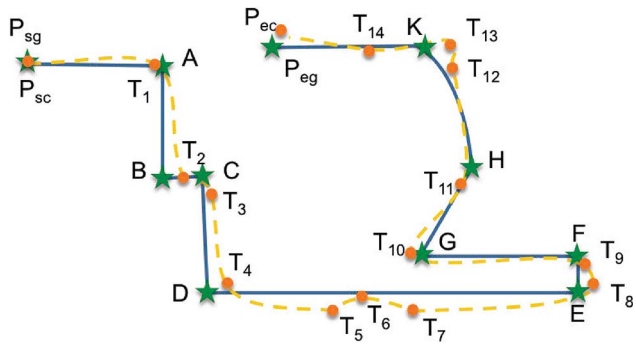

Fig. 11. A pre-planned path and the estimated trace, annotated with ground truth and estimated turns.

$$\mathcal{G} = \{P_{sg}, A, B, C, D, E, F, G, H, K, P_{eg}\}$$

and

$$\mathcal{C} = \{P_{sc}, T_1, T_2, T_3, \cdots, T_{12}, T_{13}, T_{14}, P_{ec}\}.$$

The task of turn matching is essentially to optimally match the two sequences $\mathcal{G}$ and $\mathcal{C}$.

The start and end points are directly matched and the overall length of the estimated trace is scaled to have the same length as the pre-planned path. When matching intermediate turns, there are two major sources of errors in walking trace estimation: one is walking distance errors that arise from the incorrect detection of steps or errors in step length estimation, and the other is angle detection errors due to instantaneous errors such as a hand shake, sensor drift, and imperfect walking. To consider both error sources, we define the following penalty function for matching the j^{th} turn in $\mathcal{C}$ to the i^{th} turn in $\mathcal{G}$:

$$\epsilon(i,j) = \Delta D(i,j) + \Delta A(i,j)$$

where $\Delta D(i,j) = |L_g(i) - L_c(j)|/L_g(i)$ is the relative distance difference for the i^{th} path segment, and $\Delta A(i,j) = |\angle_g i - \angle_c j|/\angle_g i$ is the relative angle difference.

With a given penalty function, the sequence matching problem can be effectively handled using dynamic programming. With the algorithm, the example in Fig. 11 would generate the following optimal matching results:

$$\{P_{sc}, T_1, T_2, T_3, T_4, -, -, -, T_8, T_9, T_{10}, T_{11}, -, T_{13}, -, P_{ec}\}$$

where "$-$" indicates a discarded candidate turn.

Magnetic Field Map Construction: After fixing the turns' positions, we calculate the location of the intermediate steps proportionally according to their estimated step length and the overall distance between two bounding turns. The location of each fingerprint is then interpolated from the locations of the two bounding steps, proportional to their time differences. The final M-Map is constructed by extrapolating the magnetic field strength on the survey path towards both sides until reaching

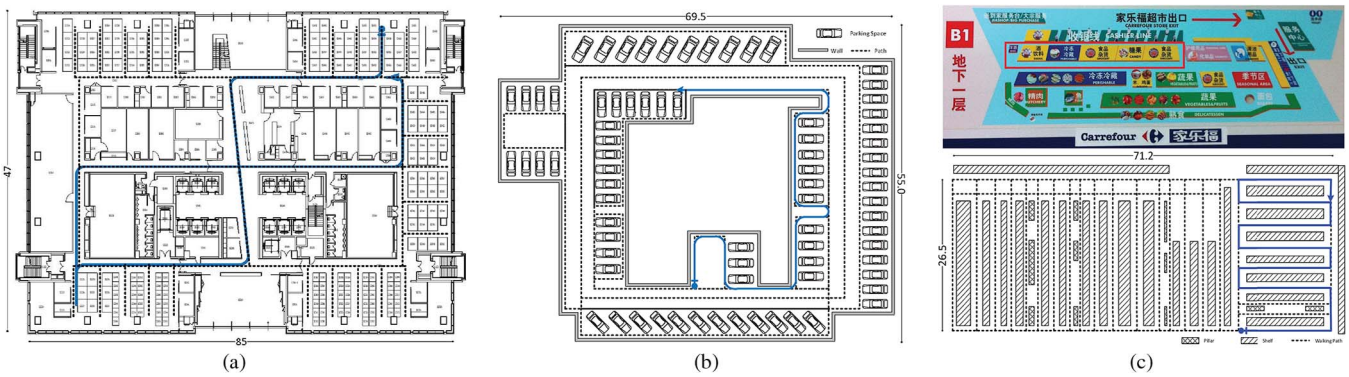

Fig. 12. Layout of the three testing environments, with data collection paths and a highlighted typical walking trace. (a) Office floor. (b) Underground parking lot. (c) Supermarket.

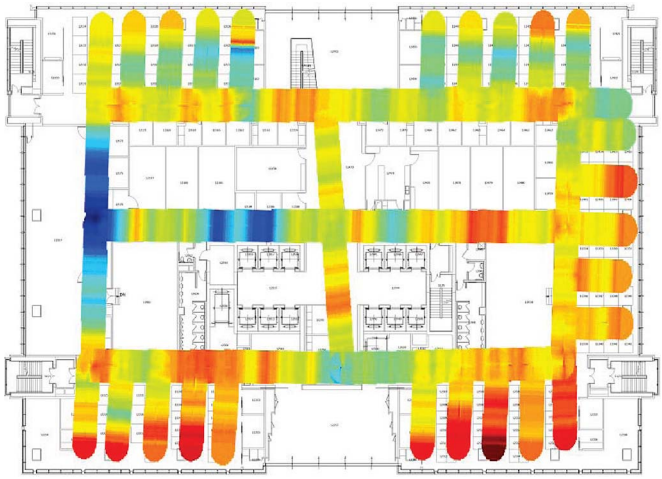

Fig. 13. Generated M-Map for an office building, overlaid on the floor plan.

the walls. For wide pathways, multiple parallel survey paths may exist. Magnetic field strengths at intermediate locations are interpolated according to their distances to each bounding path. For crossroads and turning areas, the average of the interpolated strengths (from different survey paths) is used. Fig. 13 shows the 2-D view of the resulting M-Map for an office building (refer to Fig. 12(a)), which is used in the evaluation in Section VII. From the figure, we can clearly see the locally-specific disturbances of the indoor magnetic field.

VII. System Evaluation

In this section we will first present micro-benchmark results on the key components of the Magicol system, and then evaluate the system in a variety of representative indoor environments, to understand its effectiveness and limitations. Due to space constraints, we put the evaluation of map construction and complexity and energy consumption analysis in Appendix.

A. Implementation

We implemented a Magicol client on HTC Mazaa smartphone with a 1 GHz processor and 576MB RAM, running Windows Phone 7.5, and the Magicol Cloud service on a Dell PC, with a 2.8 GHz processor and 4G RAM, running Windows 7. We adopted KLD-sampling [30] to change the number of particles on-the-fly on the basis of their distribution. The initial number of particles was 3000.

Background Data Logging: The mobile client performed continuous background IMU sampling and walking state detection [25]. When the user was detected to be walking, the step information and the magnetic field signals were logged. The IMU sampling frequency was set to 30 Hz for both the accelerometer and the magnetometer, and 50 Hz for the gyroscope. When the user issued a location query, a WiFi scan was also conducted. As will be shown later, only a short duration (e.g. 30 seconds) of the latest walking trace was usually sufficient to localize the user. Therefore, we may only need to keep a small buffer for the walking trace.

B. Localization Using Magnetic Field Only

Testing Environment and Ground Truth Acquisition: We extensively evaluated the system performance in three representative indoor environments: an office floor, an Underground Parking Lot (UPL) and a supermarket, with a testing area of about 4000 m^2, 3850 m^2, and 1900 m^2, respectively. Floor maps of the three testing environments are shown in Fig. 12, along with survey paths using dashed lines and one typical walking trace using solid lines. The supermarket was huge and we walked only a portion of it, as shown in the red rectangle in the upper picture in Fig. 12(c). Overall, we collected more than 100 indoor walking traces with a total walking distance of 25 kilometers. To obtain the ground truth of walking, we set up many landmarks and obtain their real positions in advance, and record the time (by tapping on the phone screen) when passing by those landmarks. Localization error is then obtained by computing the Euclidian distance between the estimated positions and the ground truth.

The results were compared with the Dead Reckoning (DR) based localization system [25]. Note that we have used exactly the same step detection and step length estimation techniques. Thus, the performance differences are purely due to our way of leveraging the magnetic field.

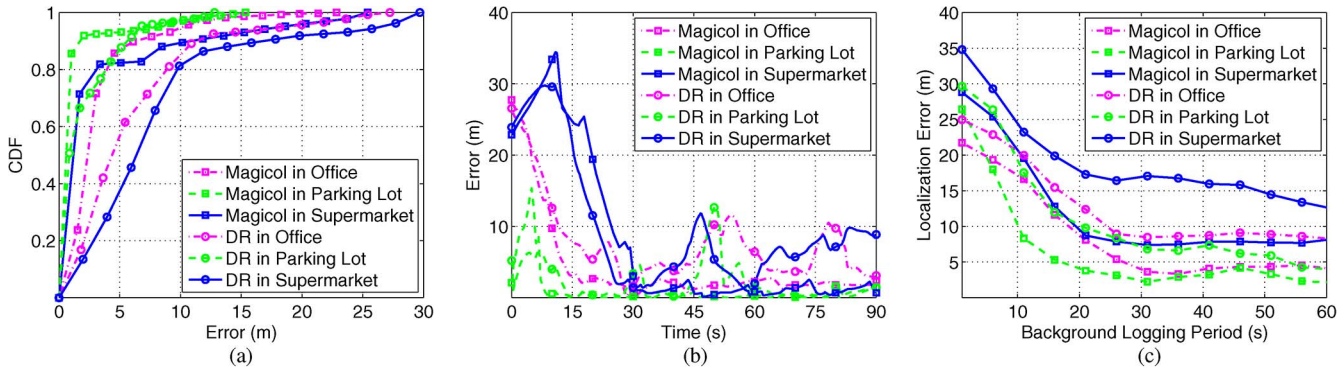

Fig. 14. Localization performance in different testing environments. (a) CDF of long traces. (b) The typical traces. (c) Error vs trace length.

Localization With Long Traces: We walked many traces in the whole area with randomly picked starting points and made random turns. These walks were relatively long, around 2 minutes. Fig. 14(a) shows the cumulative distribution function (CDF) of localization errors for the three testing environments. We can see that Magicol significantly and consistently outperformed the Dead Reckoning system for all testing environments. For the office floor, the 80 percentile error of Magicol was 4 m while it was around 9.5 m for DR; For the supermarket, performances of both Magicol and DR are still reasonably good as the 80 percentile errors were approximately 3.5 m and 10 m, respectively. However, because supermarket was a more complex and sophisticated environment, both CDF curves increased more slowly afterwards. For the UPL, Magicol achieved extremely good accuracy—the 80 percentile of error was only 1 m. This is due to the more severe magnetic field anomalies in the UPL. The accuracy of DR was also good for the UPL, and the 80 percentile error was about 4 m. The reason was due to the simple layout of the pathways.

Fig. 14(b) shows the intermediate localization results (during particle filtering) against the walking time for typical traces, for all three environments. From the figure, we can see that Magicol exhibited a steadier performance: after the initial convergence process, it rarely diverged again. But for DR, there were several spikes after the initial convergence. The reason was due to the erroneous externally sensed direction. This phenomenon indicates an interesting difference between Magicol and conventional tracking-based systems: conventional tracking-based systems rely on turns to kill unlikely particles [25], while Magicol performs equally well for straight walking traces, thanks to the continuous sensing of the magnetic field.

Localization Performance vs Trace Length: Fig. 14(b) indicates that Magicol can localize a user after about 20 seconds of walking. This suggests that we may not need to log very long motion traces. We thus evaluated the localization performance of Magicol at different logged trace lengths. We collected 5 long traces in each testing environment and randomly selected a portion of them to emulate motion traces with different lengths. Fig. 14(c) shows the average localization error at different trace lengths for both Magicol and DR for the three testing environments. We can see that Magicol typically achieved good accuracy for log lengths longer than 20 seconds and the resulting localization error was only a few meters, whereas the performance of DR was much worse even with much longer traces. As the length of logged trace has a direct impact on the execution of the augmented particle filtering (see Appendix), this indicates another advantage of Magicol over conventional DR.

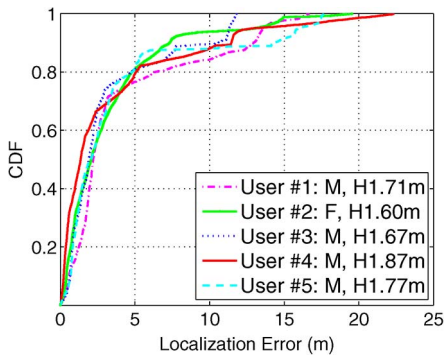

Fig. 15. Localization robustness among users.

Robustness among Different Users: The above experimental results on tracking and location accuracy were based on the traces mainly collected by two of our authors. To examine Magicol's robustness when used by other people that may have different stride lengths and walking speeds, we employed five other users (4 male and 1 female) with different heights (between 1.60 m to 1.87 m) and asked them to walk along the same path (around 40 seconds) in the office environment. The CDF of the localization error for all five users are plotted in Fig. 15. From the figure we can see that the five CDF curves are very close, and they are consistent with the experimental results from our own walks. This demonstrates the robustness and practicality of Magicol.

C. Magnetic-WiFi Fusion

Among the three testing environments, only the office floor had dense enough WiFi AP deployment that WiFi-based localization methods worked. Specifically, there was only one AP in the UPL and 3 APs in the subarea of the supermarket. This evidently showcases the pervasive applicability of Magicol. Therefore, we only studied the combination of Magicol (i.e., using normal particle filtering) and WiFi-based schemes for the office floor. We used Radar [1] and EZ [3] in our experiments.

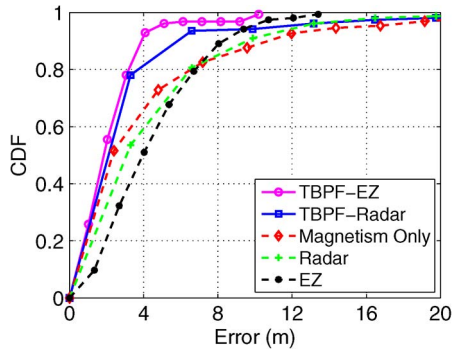

Fig. 16. Localization performance comparison.

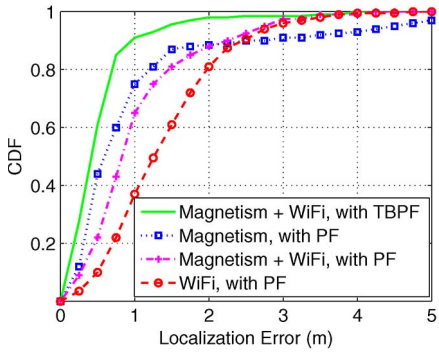

Fig. 17. Tracking performance comparison with different magnetic-WiFi fusion approaches.

RADAR is an RSS fingerprinting scheme. An incoming measurement is matched against all fingerprints in the database. We used the K-NN method ($K = 5$) to estimate location. EZ is a model-based scheme. It infers various propagation model parameters based on a large number of measurements in advance. An incoming measurement is applied to the model to obtain the estimated position. We have used the same compliant-walking method (in Section VI) to construct the M-Map and the WiFi location database, and to compute the model parameters with the same set of collected data.

Localization Accuracy with Magnetic-WiFi Fusion: Fig. 16 shows the point localization accuracy of Radar, EZ, Magicol, and when fused with WiFi using TBPF. Radar and EZ affects TBPF's performance due to different initial position. From the figure, we can see that Magicol (with a 40-second motion trace) can achieve comparable performance to Radar and EZ on its own. The combination leads to a more significant performance improvement than using any individual method. When combined with Radar, the 90 percentile accuracy was about 5.3 m, which was about a 50% improvement over that of Radar (i.e., 10.1 m). Similarly, when combined with EZ, the 90 percentile accuracy improved to 3.9 m over the original 8 m accuracy achieved using EZ only. From the figure, we can also observe that the combination is more powerful for those locations where individual method yields larger errors. This is due to the complimentary nature of magnetic and WiFi signals.

Tracking Performance With Magnetic-WiFi Fusion: We evaluate the tracking accuracy with different magnetic-WiFi fusion approaches, namely the hybrid method (Eqn. (4)) and the proposed TBPF method, where we trace back for 15 steps upon each new WiFi scan. Experiments are conducted in the office environment due to its dense WiFi deployment. For comparison purpose, we also include the performances when only magnetic field or WiFi is used in tracking (with normal PF) as benchmarks. Note that even though WiFi was continuously scanned, but it took about 2 seconds to obtain a fingerprint. Thus, there is about a 3-step interval between two subsequent fingerprints. Fig. 17 shows the performance gain of TBPF over normal PF (which is adopted in the hybrid fusion approach) when magnetic field and WiFi are combined in tracking. Compared with the 90 percentile accuracy of 2.1 m obtained by magnetism-based tracking which uses normal particle filtering only, we see that the TBPF is very effective, achieving a 57% improvement with 90 percentile accuracy of less than 1 m. The intuitive

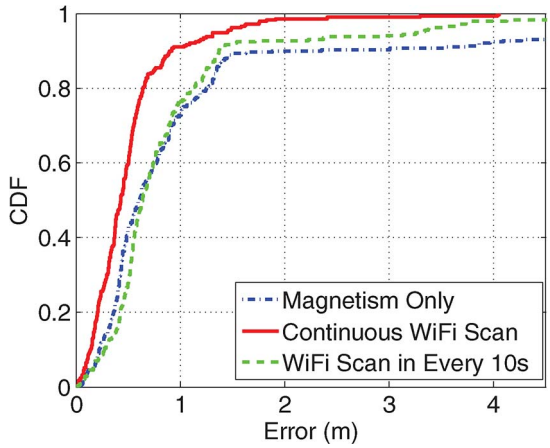

Fig. 18. Tracking performance with magnetic-WiFi fusion, with reduced WiFi sampling frequency.

hybrid performs slightly worse than using magnetism only, due to the jumpy nature of WiFi signal, but does help to suppress large errors. We animated and visually examined the tracking process of some traces and found that the resulting distribution of TBPF is significantly more concentrated than the cases of single pass particle filtering. Compare against Fig. 16, we found that tracking accuracy significantly outperforms that of point localization. It is reasonable due to the constraint imposed by dead reckoning between subsequent WiFi scans. The cost we pay is extra energy consumed by multiple WiFi scans.

To see the impact of WiFi scan frequency, we also tried to scan WiFi less frequently at roughly 10 seconds intervals (about 15 steps). The results are shown in Fig. 18. We can see that the performance drops quickly, almost to that of using magnetic field only. It is expected as most of steps do not have a WiFi fingerprint. However, it is still helpful in confining relatively larger errors.

As a final remark, Magicol was initially implemented and evaluated on a Windows Phone. We have applied this technology in Travi-Navi [31] and also evaluated on a variety of Android mobile devices (including Samsung Galaxy S2, S4, Note3, HTC Desire and HTC Droid Incredible 2). The results there confirmed that the design of Magicol is intrinsically immune to device diversities due to its leverage of the shape instead of the absolute sensed value of magnetic field.

VIII. Related Work

Indoor localization is an extensively studied topic, mostly relying on certain infrastructure, and WiFi is mostly explored [1]–[4], [19], [20], [32]. We only review closely related work here.

IMU-Based Tracking: IMU-tracking (a.k.a., Dead Reckoning) is a well-studied topic for its infrastructure independency [10], [25], [33]–[35]. These systems handle the noisy walking directions caused by locally disturbed indoor magnetic field through fusion with gyroscope readings to obtain compromised heading directions. A map is usually used to constrain the tracking error. In contrast, Magicol exploits the magnetic field anomalies as useful features, and makes *separate use* of the gyroscope and the magnetometer. Magicol makes more use of the map for not only constraining the motion but also initializing directions of particles.

Magnetism-Based Localization: Geomagnetism was exploited for localization [21] or tracking purpose in the robotics field using special hardware, [15], [16], [36], [37]. However, these techniques either requires dense samples of magnetic vector which leads to tedious training overhead [21], or incur special hardware or draw on existing tracking techniques (e.g., odometric) which are not applicable to off-the-shelf smartphones (e.g., due to unpredictable human behaviors, we do not know the heading direction and can no longer use magnetic output from X, Y, Z axis independently).

For smartphones, the geomagnetic field anomalies were leveraged in a leader-follower scenario [13], [22]. In [23], the authors leveraged observations of the ambient magnetic field, but they only handled simple one-dimensional (e.g., in a straight pathway) situations and did not handle many practical problems such as the various diversities that Magicol does. In [38], Glanzer *et al.* introduce a pedestrian navigation system with human motion recognition. However, the pre-mapped magnetic field information is only used to correct the severe disturbance of indoor direction sensing. In [39], authors leverage magnetic signatures to identify locations and rooms. Although mobile phones are used to measure magnetic field intensity, the system relies on pillars and only offers rough positioning result (e.g. room-level). Kim *et al.* explored geomagnetism for indoor localization in rather simplistic settings—a single corridor in a building, and assumed known user motion and the starting point [17]. Grand *et al.* [24] propose a light-weight magnetic map construction method and use online particle filter to estimate the location of the handheld device. However authors mainly emphasis the disturbance of magnetic field whereas in Magicol, we jointly consider efficient database construction, dynamic user motion behaviors, limited discernibility of magnetic field, and run the localization algorithm in a real-time manner. In addition, we further enhance Magicol using complementary WiFi-based techniques at low energy cost.

Location Database Construction: SLAM has been heavily studied in the robotics field [26]. FootSLAM [11] used shoe-mounted inertial sensors to construct the internal map for an unknown building. Zee [19] studied the same problem for mobile users using a crowdsourcing approach. Unloc [12] explored various types of natural landmarks detectable from sensor readings to calibrate user traces. These methods usually suffer from poor initial accuracy of the mapping, and take long time to reach an acceptable accuracy. In contrast, our compliant-walking based approach aims at improving the efficiency (essentially, any path needs only one visit) and, at the same time, lowers the bar for site surveyors as they just need to walk along a given path.

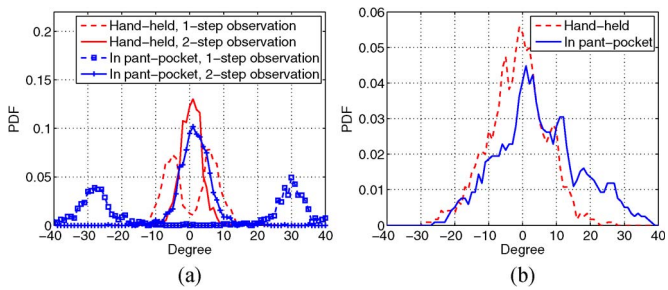

Fig. 19. Relative walking direction estimation using gyroscope at different device attitudes. (a) Walking straight. (b) Turning cases.

IX. Conclusion

In this paper, we present Magicol, a pervasive and practical, geomagnetism-based indoor localization system. We conducted a comprehensive study of the indoor magnetic field and designed Magicol with minimal assumptions. Magicol uses an efficient compliant-walking-based data collection method for database construction, and addresses all challenges that arise from the magnetic field. In addition, we propose methods for combining Magicol with infrastructure (WiFi)-based localization methods to further improve accuracy. We implemented Magicol on off-the-shelf smartphones and evaluated it in three typical indoor environments and among different users. The experimental results confirm the effectiveness and high accuracy of Magicol.

Appendix

A. Map Construction Evaluation

a) Relative walking direction detection: Fig. 19 shows the error distribution of the relative walking direction using a gyroscope, with the device held at different body positions, namely hand-held and in a pants pocket. We experimented with both straight walking and turning cases. One interesting observation from Fig. 19(a) is that people tend to have symmetric direction changes at every other step, which is more obvious when the device is put in a pants pocket, due to the natural balance of human walking. This suggests we should use the average of two consecutive steps as the actual relative direction. The resulting error is usually within several degrees when walking straight. For the turning cases, we do not see the symmetric pattern as we accumulate the turning angle from all the steps in a turn. The resulting estimation error is slightly larger than when walking but is well below 20 degrees, as shown in Fig. 19(b).

b) Trace matching for compliant-walking: The performance of the user trace estimation and turn matching algorithm does not depend on any environmental factor but rather on how

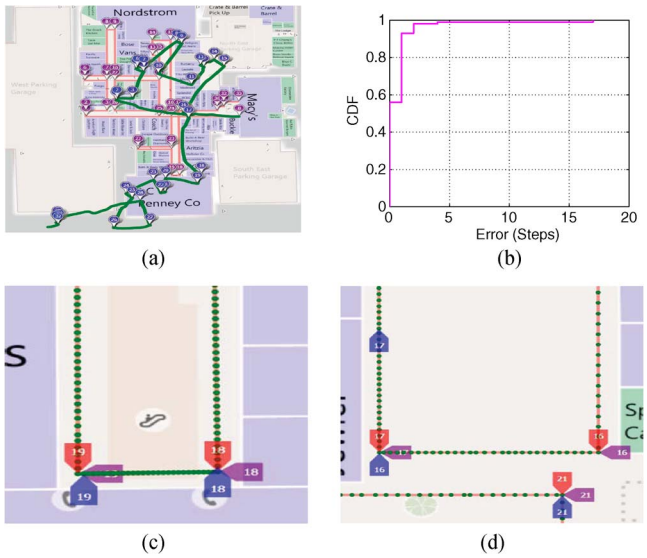

Fig. 20. Experimental results on turn matching. (a) Plan and user trace. (b) CDF of matching error. (c) Wrong map scale. (d) Wrong user tapping.

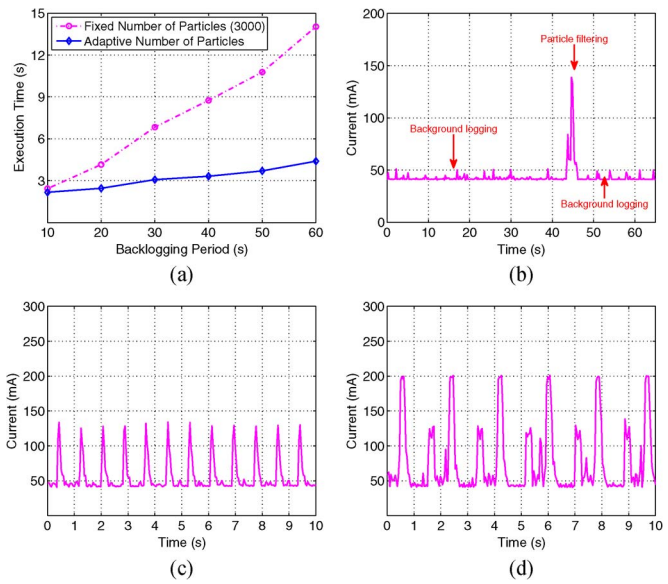

Fig. 21. Execution time and energy profiling. (a)Execution time vs log length. (b) Magicol localization. (c) Magicol tracking. (d) WiFi (EZ) tracking.

compliantly the surveyor walks and the accuracy of the map. We conducted experiments in both an office building and a large shopping mall. The office environment turned out to be very easy as narrow corridors force sharp turns. Here we only present the results from the shopping mall. We planned two paths, each with 32 turns. Three volunteers walked twice for each path. Thus we have 12 traces and the total walking time was about 3 hours. To collect the ground truth, we asked the user to tap on the phone when turning.

Fig. 20(a) shows one pre-planned path with ground truth turns and an estimated trace with user marked turns. Fig. 20(b) shows the accumulated distribution of the distance error between matched turns and those marked by users in unit of steps. Each step is around 0.8 meters on average. About 90% of the matched turns were within one step from the user marks, and 98% were within five steps. However, there were a few turns that had larger errors. By examining the penalty function for all resulting path segments, we easily identified these "wrong" turns. The results show that some of the mistakes were actually due to the wrong map scale in the proximity of two specific turns (first figure in Fig. 20(c)). The largest error occurred because the user forget to mark a turn and marking an incorrect one afterwards to remedy the mistake. It is shown in Fig. 20(c) where turn 16 was delayed and turn 17 marked at the wrong location.

B. Complexity and Energy Consumption

Energy consumption is more of a concern when continuous localization (i.e., tracking) is required. The Magicol client may work in online or offline mode. It is more energy efficient to pre-download the M-Map with the indoor map, either in advance or during the first online location query to the service, and then operate in the offline mode afterwards. In this part, we recorded the measurements of system complexity and energy consumption for the offline mode, where all the computations happened on the device.

a) Execution time of location inference: The execution time of a location fix on the mobile client (offline mode) for traces with different lengths is shown in Fig. 21(a). The initial particle number was set to 3000. Except for a constant initial startup delay, we observe a linear relationship between the execution time and the length of the walking trace. Fig. 21(a) also shows the effect of the adaptive particle number, as a system optimization technique (we used KLD-sampling [41]): the processing time decreases significantly. For example it took about 3 seconds to process a 40 s walking trace, which was about one third of the execution time if the particle number was fixed to 3000. Real-time tracking was easily achievable as it took only 0.06 s on average to perform the particle filtering for one step. Using WiFi at the same time would lead to a further shortened delay due to the faster convergence of particles.

b) Energy consumption of location fix and tracking: We used a Power Monitor [43] to measure current and quantify the energy consumption of Magicol. Fig. 21(b) shows the runtime current of the Magicol client in online mode for a typical localization process using only magnetic signal. There are two main operating states: background logging (till 43 s and after 46 s) and particle filtering (44 s–46 s), and they consumed about 42 mA and 140 mA, respectively. Note that there were small spikes in the background logging period, due to the light weight step detection.

Fig. 21(c) shows the energy consumption of the Magicol client running in offline mode for a continuous tracking process. Magicol was executed at every step, and consumed about 135 mA for about 0.1 seconds, which was about 49 mJ energy per location fix. In order to compare, we also show the energy consumption for WiFi-based tracking (using the EZ method, with the model database pre-downloaded) in Fig. 21(d). For each location fix, it took about 0.4 seconds for WiFi scanning (active scan), which consumed about 200 mA current and 0.35 seconds for location resolving that consumes 125 mA

current. Thus, the rough energy consumption was about 445.5 mJ per location fix. Therefore, Magicol tracking was 9× more energy efficient than WiFi-based tracking.

c) Energy consumption of background data logging: In current smartphones, background data logging needs to activate the main CPU and thus consumes more energy than necessary. The IMU sensor themselves consumes negligible energy. For example, LSM330DLC uses about 11 uA and 6.1 mA at highest rate for the accelerometer and gyroscope, respectively. They drop to 6 uA and 2 mA in low power mode [45]. The AK8975c compass consumes about 0.35mA at a high sampling rate [40]. The computational complexity of sensor sampling and walking state detection is also simple. A low power MCU such as MSP430 series can do the job, and consumes only a few milliamperes [46]. Actually, given the high demand of continuous sensing of user contexts (including motion states) by many mobile applications, future mobile phones may have more energy-efficient peripheral sensory boards [42], [44] and a new CPU design (e.g., [47]) that can dedicate one core for all the low energy sensing tasks. Thus background data logging will be affordable and amortized among multiple applications.

REFERENCES

[1] P. Bahl and V. N. Padmanabhan, "RADAR: An in-building RF-based user location and tracking system," in *Proc. IEEE INFOCOM*, 2000, pp. 775–784.

[2] M. Youssef and A. K. Agrawala, "The Horus WLAN location determination system," in *Proc. ACM MobiSys*, 2005, pp. 205–218.

[3] K. Chintalapudi, A. P. Iyer, and V. N. Padmanabhan, "Indoor localization without the pain," in *Proc. ACM MobiCom*, 2010, pp. 173–184.

[4] J. Xiong and K. Jamieson, "ArrayTrack: A fine-grained indoor location system," in *Proc. USENIX NSDI*, 2013, pp. 71–84.

[5] J. Paek, K.-H. Kim, J. P. Singh, and R. Govindan, "Energy-efficient positioning for smartphones using Cell-ID sequence matching," in *Proc. ACM MobiSys*, 2011, pp. 293–306.

[6] Q. Xu, A. Gerber, Z. M. Mao, and J. Pang, "AccuLoc: Practical localization of performance measurements in 3G networks," in *Proc. ACM MobiSys*, 2011, pp. 183–196.

[7] J. Yang, A. Varshavsky, H. Liu, Y. Chen, and M. Gruteser, "Accuracy characterization of cell tower localization," in *Proc. ACM Ubicomp*, 2010, pp. 223–226.

[8] Y. Chen, D. Lymberopoulos, J. Liu, and B. Priyantha, "FM-based indoor localization," in *Proc. ACM MobiSys*, 2012, pp. 169–182.

[9] S. Yoon, K. Lee, and I. Rhee, "FM-based indoor localization via automatic fingerprint DB construction and matching," in *Proc. ACM MobiSys*, 2013, pp. 207–220.

[10] O. Woodman and R. Harle, "Pedestrian localisation for indoor environments," in *Proc. ACM UbiComp*, 2008, pp. 114–123.

[11] M. Angermann and P. Robertson, "FootSLAM: Pedestrian simultaneous localization and mapping without exteroceptive sensors—Hitchhiking on human perception and cognition," *Proc. IEEE*, vol. 100, no. Special Centennial Issue, pp. 1840–1848, May 2012.

[12] H. Wang *et al.*, "No need to war-drive: Unsupervised indoor localization," in *Proc. ACM MobiSys*, 2012, pp. 197–210.

[13] T. H. Riehle *et al.*, "Indoor magnetic navigation for the blind," in *Proc. IEEE EMBC*, 2012, pp. 1972–1975.

[14] B. Li, T. Gallagher, A. G. Dempster, and C. Rizos, "How feasible is the use of magnetic field alone for indoor positioning?" in *Proc. IPIN*, 2012, pp. 1–9.

[15] J. Chung *et al.*, "Indoor location sensing using geo-magnetism," in *Proc. ACM MobiSys*, 2011, pp. 141–154.

[16] S. Suksakulchai, S. Thongchai, D. M. Wilkes, and K. Kawamura, "Mobile robot localization using an electronic compass for corridor environment," in *Proc. IEEE ICSMC*, 2000, pp. 3354–3359.

[17] S.-E. Kim, Y. Kim, J. Yoon, and E. S. Kim, "Indoor positioning system using geomagnetic anomalies for smartphones," in *Proc. IPIN*, 2012, pp. 1–5.

[18] P. Zhou, Y. Zheng, Z. Li, M. Li, and G. Shen, "IODetector: A generic service for indoor outdoor detection," in *Proc. ACM SenSys*, 2012, pp. 113–126.

[19] A. Rai, K. K. Chintalapudi, V. N. Padmanabhan, and R. Sen, "Zee: Zero-effort crowdsourcing for indoor localization," in *Proc. ACM MobiCom*, 2012, pp. 293–304.

[20] Z. Yang, C. Wu, and Y. Liu, "Locating in fingerprint space: Wireless indoor localization with little human intervention," in *Proc. ACM MobiCom*, 2012, pp. 269–280.

[21] M. Angermann, M. Frassl, M. Doniec, B. J. Julian, and P. Robertson, "Characterization of the indoor magnetic field for applications in localization and mapping," in *IEEE IPIN*, 2012, pp. 1–9.

[22] W. Storms, J. Shockley, and J. Raquet, "Magnetic field navigation in an indoor environment," in *Proc. IEEE UPINLBS*, 2010, pp. 1–10.

[23] J. Haverinen and A. Kemppainen, "A global self-localization technique utilizing local anomalies of the ambient magnetic field," in *Proc. IEEE ICRA*, 2009, pp. 3142–3147.

[24] E. Le Grand and S. Thrun, "3-Axis magnetic field mapping and fusion for indoor localization," in *Proc. IEEE MFI*, 2012, pp. 358–364.

[25] F. Li *et al.*, "A reliable and accurate indoor localization method using phone inertial sensors," in *Proc. ACM UbiComp*, 2012, pp. 421–430.

[26] S. Thrun, W. Burgard, and D. Fox, *Probabilistic Robotics*. Cambridge, MA, USA: MIT Press, 2005.

[27] Amazon.com.Inc, Amazon Mechanical Turk. [Online]. Available: https://www.mturk.com/

[28] Wikipedia, Wall Follower. [Online]. Available: http://en.wikipedia.org/wiki/Maze_solving_algorithm

[29] Wikipedia, NED Frame. [Online]. Available: http://en.wikipedia.org/wiki/North_East_Down

[30] D. Fox, "KLD-Sampling: Adaptive Particle Filters," in *Proc. NIPS*, 2001, pp. 1–8.

[31] Y. Zheng *et al.*, "Travi-Navi: Self-deployable indoor navigation system," in *Proc. ACM MobiCom*, 2014, pp. 471–482.

[32] Y. Shu *et al.*, "Demo: G-Loc: Indoor localization leveraging gradient-based fingerprint map," in *Proc. IEEE INFOCOM*, 2014, pp. 129–130.

[33] L. Klingbeil and T. Wark, "A wireless sensor network for real-time indoor localisation and motion monitoring," in *Proc. IEEE IPSN*, 2008, pp. 39–50.

[34] I. Constandache, R. R. Choudhury, and I. Rhee, "Towards mobile phone localization without war-driving," in *Proc. IEEE INFOCOM*, 2010, pp. 1–9.

[35] C. Bo *et al.*, "Poster: Smartloc: Push the limit of the inertial sensor based metropolitan localization using smartphone," in *Proc. ACM MobiCom*, 2013, pp. 195–198.

[36] I. Vallivaara, J. Haverinen, A. Kemppainen, and J. Roning, "Simultaneous localization and mapping using ambient magnetic field," in *Proc. IEEE MFI*, 2010, pp. 14–19.

[37] S. A. Rahok and O. Koichi, "Odometry correction with localization based on landmarkless magnetic map for navigation system of indoor mobile robot," in *Proc. ICARA*, 2009, pp. 572–577.

[38] G. Glanzer and U. Walder, "Self-contained indoor pedestrian navigation by means of human motion analysis and magnetic field mapping," in *Proc. WPNC*, 2010, pp. 303–307.

[39] B. Gozick, K. P. Subbu, R. Dantu, and T. Maeshiro, "Magnetic maps for indoor navigation," *IEEE Trans. Instrum. Meas.*, vol. 60, no. 12, pp. 3883–3891, Dec. 2011.

[40] Asahi.Kasei.Microdevices.Corp. LSM330DLC Datasheet. [Online]. Available: http://www.asahi-kasei.co.jp/akm/en/product/ak8975bc/ak8975bc.html

[41] D. Fox. KLD-Sampling: Adaptive Particle Filters. In NIPS, 2001.

[42] X. Jiang and J. A. Stankovic. SEPTIMU: continuous in-situ human wellness monitoring and feedback using sensors embedded in earphones. In ACM IPSN, 2012.

[43] Monsoon.Solutions.Inc. Power Monitor. [Online]. Available: http://www.msoon.com/LabEquipment/PowerMonitor/

[44] B. Priyantha, D. Lymberopoulos, and J. Liu. Enabling energy efficient continuous sensing on mobile phones with littlerock. In ACM IPSN, 2010.

[45] STMicroelectronics.Inc. LSM330DLC Datasheet. [Online]. Available: http://www.st.com/st-web-ui/static/active/en/resource/technical/document/datasheet/DM00037200.pdf

[46] Texas.Instruments.Inc. MSP430 Datasheet. [Online]. Available: http://www.ti.com/lit/ug/slau049f/slau049f.pdf

[47] Texas.Instruments.Inc. TMS320C6472 Datasheet. [Online]. Available: http://www.ti.com/lit/wp/spry130/spry130.pdf

Yuanchao Shu (S'12) is pursuing the Ph.D. degree at State Key Laboratory of Industrial Control Technology, Zhejiang University. From 2013 to 2015, he was a joint Ph.D. student in computer science at the University of Michigan, Ann Arbor, MI, USA. He is the author and co-author of over 10 papers in premier journals and conferences, and is the recipient of the IBM Ph.D. Fellowship and the INFOCOM'14 Best Demo Award. His research interests include cyber-physical systems, mobile computing and wireless sensor network. He is a student member of ACM.

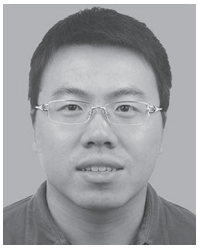

Cheng Bo received the B.E. and M.S. degrees from the Department of Computer Science, Hangzhou Dianzi University. He is currently pursuing the Ph.D. degree at the University of North Carolina at Charlotte, and is also a joint member of Wireless Network Lab, Department of Computer Science, Illinois Institute of Technology. His research interests include localization, mobile networking and computing, wireless networks, security and privacy.

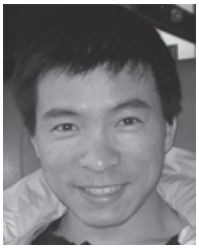

Guobin Shen (SM'06) received the Ph.D. degree in electrical engineering from the Hong Kong University of Science and Technology, Hong Kong, in 2001.

He is now a Lead Researcher with the Wireless and Networking Group, Microsoft Research Asia, Beijing, China. His current research focuses on mobile sensing and actuation systems, mobile multimedia, and low-latency mobile-cloud systems, while he has worked on topics in peer-to-peer networking and systems, wireless sensor networks, video compression and streaming, and GPU acceleration of video signal processing.

Chunshui Zhao received the bachelor's and master's degrees from Tianjin University in 1998 and 2004, respectively, and the Ph.D. degree from the Institute of Automation, China Academy of Sciences. He joined Microsoft Research Asia in July 2009. He is now a Researcher with the Mobile and Sensing Systems Group and with particular interest in fusing hardware and software techniques to build real-world systems. His current research area is indoor localization algorithms and systems.

Liqun Li received the B.E. degree from the Department of Computer Science and Technology, Tsinghua University in 2006 and the Ph.D. degree in computer science from the Institute of Software Chinese Academy of Sciences in 2012. His research interest spreads across topics related to low-power networking, indoor localization, and mobile sensing systems. He is a Senior Software Engineer at PPzuche.com. Before that, he was an Associate Researcher in the Mobile and Sensing System Group (MASS), Microsoft Research Asia from 2012 to 2014.

Feng Zhao (F'10) received the B.S. degree from Shanghai Jiaotong University in 1984, and the M.S. and Ph.D. degrees in electrical engineering and computer science from MIT in 1988 and 1992, respectively. He taught at Ohio State University as an Assistant and then tenured Associate Professor in Computer Science (1992–1997), and at Stanford University as a Consulting Professor of Computer Science (1999–2006). He is also a Professor at Shanghai Jiaotong University, University of Science and Technology of China, and Harbin Institute of Technology, and an Affiliate Faculty at University of Washington. He serves on the advisory boards for Information Engineering at Chinese University of Hong Kong and Computer Science and Engineering at Hong Kong University of Science and Technology. He is an Assistant Managing Director at Microsoft Research Asia, responsible for the hardware, mobile and sensing, software analytics, systems, and networking research areas. His research has focused on wireless sensor networks, energy-efficient computing, and mobile and cloud systems. He has authored or co-authored over 100 technical papers and books, including the book, *Wireless Sensor Networks: An information processing approach* (Morgan Kaufmann), and has over 30 US patents issued.

Since joining Microsoft Research Asia in 2009, he and his team have developed mobile and cloud solutions that advanced the state-of-the-art in computing and significantly impacted Microsoft product groups: accurate indoor navigation system, efficient search index serving platform, interactive visual analytics for big data, and software defined radio and networking for data centers.

Prior to joining MSR-Asia, he was a Principal Researcher at Microsoft Research Redmond (2004–2009), and founded the Networked Embedded Computing Area. During this time, he led the team to develop the MSR sensor mote, Tiny Web Service, SenseWeb and SensorMap, Data Center Genome, JouleMeter, and GAMPS data compression. With the help of some of these technologies, Microsoft data centers are considered among the most densely instrumented and monitored cloud computing infrastructures in the world.

He was a Principal Scientist at Xerox Palo Alto Research Center (Xerox PARC)(1997–2004) and founded PARC's sensor network effort. He played a key role in PARC's Smart Matter Project that developed tiny networked sensors and actuators for embedding into physical environments, and a suite of collaborative sensing, control and processing protocols, including the IDSQ algorithm.

Dr. Zhao was the founding Editor-In-Chief of *ACM Transactions on Sensor Networks* (2003–2010), and founded the ACM/IEEE IPSN conference in 2001. He served on the ACM SIGBED Executive Committee (2004–2010), as Technical Program Co-Chair for ACM Sensys'05 and Mobisys'13, and on the Steering Committee for CPSWeek (2007-present). In 2008, he worked with USENIX and ACM to start HotPower, a technical forum focusing on sustainable computing. He received a Sloan Research Fellowship (1994) and US NSF and ONR Young Investigator Awards (1994 and 1997). His work has been featured in news media such as *BBC World News*, *BusinessWeek*, and *Technology Review*.